



THE UNIVERSITY *of* EDINBURGH

Edinburgh Research Explorer

The clinical utility of hybrid imaging for the identification of vulnerable plaque and vulnerable patients

Citation for published version:

Bing, R, Driessen, RS, Knaapen, P & Dweck, MR 2019, 'The clinical utility of hybrid imaging for the identification of vulnerable plaque and vulnerable patients', *Journal of Cardiovascular Computed Tomography*. <https://doi.org/10.1016/j.jcct.2019.07.002>

Digital Object Identifier (DOI):

[10.1016/j.jcct.2019.07.002](https://doi.org/10.1016/j.jcct.2019.07.002)

Link:

[Link to publication record in Edinburgh Research Explorer](#)

Document Version:

Publisher's PDF, also known as Version of record

Published In:

Journal of Cardiovascular Computed Tomography

General rights

Copyright for the publications made accessible via the Edinburgh Research Explorer is retained by the author(s) and / or other copyright owners and it is a condition of accessing these publications that users recognise and abide by the legal requirements associated with these rights.

Take down policy

The University of Edinburgh has made every reasonable effort to ensure that Edinburgh Research Explorer content complies with UK legislation. If you believe that the public display of this file breaches copyright please contact openaccess@ed.ac.uk providing details, and we will remove access to the work immediately and investigate your claim.



Accepted Manuscript

The clinical utility of hybrid imaging for the identification of vulnerable plaque and vulnerable patients

Rong Bing, Roel S. Driessen, Paul Knaapen, Marc R. Dweck

PII: S1934-5925(19)30085-1

DOI: <https://doi.org/10.1016/j.jcct.2019.07.002>

Reference: JCCT 1319

To appear in: *Journal of Cardiovascular Computed Tomography*

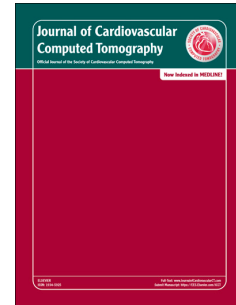
Received Date: 15 February 2019

Revised Date: 3 May 2019

Accepted Date: 7 July 2019

Please cite this article as: Bing R, Driessen RS, Knaapen P, Dweck MR, The clinical utility of hybrid imaging for the identification of vulnerable plaque and vulnerable patients, *Journal of Cardiovascular Computed Tomography* (2019), doi: <https://doi.org/10.1016/j.jcct.2019.07.002>.

This is a PDF file of an unedited manuscript that has been accepted for publication. As a service to our customers we are providing this early version of the manuscript. The manuscript will undergo copyediting, typesetting, and review of the resulting proof before it is published in its final form. Please note that during the production process errors may be discovered which could affect the content, and all legal disclaimers that apply to the journal pertain.



Journal of Cardiovascular Computed Tomography

Review article

The Clinical Utility of Hybrid Imaging for the Identification of Vulnerable Plaque and Vulnerable Patients

Short title: Hybrid imaging of vulnerable plaque

Rong Bing¹ MBBS, Roel S Driessen² MD, Paul Knaapen² MD PhD, Marc R Dweck¹ MD PhD

¹ BHF Centre for Cardiovascular Science, University of Edinburgh, 47 Little France Crescent, Edinburgh, United Kingdom

² Department of Cardiology, VU University Medical Centre, de Boelelaan 1117 1081 HV Amsterdam, The Netherlands

Word count: 4783

Disclosures: No disclosures

Address for correspondence:

Dr Marc R Dweck

BHF Centre for Cardiovascular Science, University of Edinburgh

47 Little France Crescent

Edinburgh EH16 4TJ

Tel: +44 131 242 6515

Email: Marc.dweck@ed.ac.uk

Twitter: @MarcDweck

1 ABSTRACT

2 Despite decades of research and major innovations in technology, cardiovascular
3 disease remains the leading cause of death globally. Our understanding of major
4 cardiovascular events and their prevention is centred around the atherosclerotic
5 plaque and the processes that ultimately lead to acute plaque rupture. Recent
6 advances in hybrid imaging technology allow the combination of high spatial
7 resolution and anatomical detail with molecular assessments of disease activity. This
8 provides the ability to identify vulnerable plaque characteristics and differentiate
9 active and quiescent disease, with the potential to improve patient risk stratification.
10 Combined positron emission tomography and computed tomography is the
11 prototypical non-invasive hybrid imaging technique for coronary artery plaque
12 assessment. In this review we discuss the current state of play in the field of hybrid
13 coronary atherosclerosis imaging.

14

15 **KEYWORDS**

16 Vulnerable plaque

17 Atherosclerosis

18 Computed tomography coronary angiography

19 Myocardial perfusion

20 Positron emission tomography

21 Fractional flow reserve

22 Coronary physiology

23

24 **ABBREVIATIONS**

25 CMR Cardiac magnetic resonance

26 CT Computed tomography

27 CTCA Computed tomography coronary angiography

28 FFR Fractional flow reserve

29 FFR_{CT} Computed tomography coronary angiography-derived fractional flow
30 reserve

31 MRCA Magnetic resonance coronary angiography

32 PET Positron emission tomography

33

34 INTRODUCTION

35 Cardiovascular disease is the leading cause of death globally, despite advances in
36 risk stratification, diagnostic tools and preventative therapies (1). Consequently,
37 there remains major interest in refining our current methods of diagnosis and risk
38 stratification to better individualise preventative therapies. Myocardial infarction is
39 most commonly caused by rupture of atherosclerotic plaque. Plaques that are prone
40 to rupture have certain common characteristics that together define the vulnerable
41 plaque. Vulnerable plaques have played an integral role in our understanding of
42 atherosclerosis and cardiovascular disease, with extensive research conducted to
43 better characterise and identify these lesions (2). However, appreciation of the fact
44 that the majority of vulnerable plaques ruptures are clinically silent has led to a
45 paradigm shift in atherosclerotic plaque imaging; focus has shifted from the level of
46 the individual plaque to the patient (3), and from invasive to non-invasive imaging
47 modalities. This change has coincided with advances in non-invasive imaging
48 techniques which now facilitate comprehensive assessments of plaque
49 characteristics and disease activity across the coronary vasculature. Hybrid
50 cardiovascular imaging is at the frontier of clinical research in this field, although it
51 has yet to become adopted for routine clinical use.

52

53 HYBRID IMAGING: RATIONALE AND CONCEPTS

54 The pathophysiology of atherosclerosis and the vulnerable plaque is well-described
55 (2). There are hallmarks characteristics of high-risk plaque that have been identified
56 on histology, invasive intracoronary imaging and computed tomography coronary
57 angiography (CTCA) which serve as specific targets for hybrid coronary imaging.
58 The prototypical thin-cap fibroatheroma features inflammation (predominantly

59 macrophage infiltration), a large lipid-rich necrotic core, a thin fibrous cap (<65 μm),
60 superficial microcalcification and plaque haemorrhage. Notably, these findings are
61 independent of stenosis severity; myocardial infarction is often due to plaque rupture
62 in non-obstructive lesions (4, 5). As our ability to image these plaques has improved
63 it has become clear that the majority of these lesions appear to either heal or rupture
64 sub-clinically with only very few leading to myocardial infarction. In the landmark
65 PROSPECT trial (4), 596 thin-cap fibroatheromas were identified on virtual-histology
66 intravascular ultrasound (IVUS) in a cohort of 697 patients with acute coronary
67 syndrome. After 3 years' follow-up, only 31 myocardial infarctions, cardiac arrests or
68 cardiac deaths occurred. Of these, 14 were related to the original culprit lesion. The
69 recent Lipid Rich Plaque study demonstrated that the lipid core burden index on
70 near-infrared spectroscopy IVUS predicted both culprit and non-culprit major adverse
71 cardiovascular events at 24 months (6). The value of invasive assessments of
72 plaque morphology and plaque-directed therapies has therefore been questioned.
73 Vulnerable plaque assessment appears to be of greater value at the level of the
74 patient, using non-invasive imaging to interrogate the entire coronary vasculature.
75 Those subjects in whom adverse plaque characteristics are identified are at
76 increased risk of future events, although the originally identified lesion may not itself
77 result in a clinical event. As such, total atherosclerotic burden has yet to be
78 superseded for prognostic purposes by any plaque-level imaging (3).

79

80 Hybrid imaging techniques combine two different modalities, taking advantage of
81 their individual strengths to provide a comprehensive dataset. A modality with high
82 temporal and spatial resolution is required to provide anatomical detail and
83 assessments of soft tissue composition. For the coronary arteries, the most common

84 of these is CTCA, although cardiovascular magnetic resonance (CMR) can also be
85 utilised. For hybrid coronary plaque assessment, this dataset is most commonly
86 fused with positron emission tomography (PET). This allows interrogation of plaque
87 biology and potentially any disease process but requires appropriately targeted
88 radiotracers. The ability of hybrid PET-CT and PET-MR to provide this breadth of
89 information about anatomy, plaque composition and disease activity make them
90 exciting techniques with which to study coronary atherosclerosis.

91

92 **HYBRID IMAGING: PLAQUE CHARACTERISTICS**

93 Non-invasive imaging of vulnerable plaque morphology has been extensively studied
94 with CT and MR as described below.

95

96 **Computed tomography coronary angiography**

97 CTCA has been at the forefront of coronary plaque characterisation for many years,
98 with studies demonstrating close correlation between CTCA and intravascular
99 imaging findings of thin-cap fibroatheromas (7, 8). There are several classic CTCA
100 features of vulnerable plaque: low-attenuation (<30 Hounsfield Units), positive
101 remodelling (commonly defined as a remodelling index >1.1), spotty calcification and
102 the napkin-ring sign (low-attenuation plaque core with a rim of higher attenuation).
103 Early data from Motoyama *et al* described the increased prevalence of low
104 attenuation plaque (79% vs 9%), positive remodelling (87% vs 12%) and spotty
105 calcification (63% vs 21%) in culprit lesions compared to stable lesions (9). Further
106 prospective data demonstrated an increased rate of acute coronary syndromes in
107 patients with high-risk plaque (16.3% vs 1.4% at mean follow-up of 3.9 ± 2.4 years,
108 hazard ratio [HR] 8.24 (95% confidence interval [CI] 5.26 – 12.96)) (10). There now

109 exists a large body of non-randomised evidence supporting these findings (5, 9-12).
110 Recent analyses from the two largest randomised trials of CTCA in symptomatic
111 patients with suspected stable coronary artery – the Prospective Multicenter Imaging
112 Study for Evaluation of Chest Pain (PROMISE) and Scottish Computed Tomography
113 of the Heart (SCOT-HEART) trials – have added further weight to the prognostic
114 power of CTCA assessments of vulnerable plaque. In PROMISE, 676 (15%) patients
115 had high-risk plaque, conferring a greater risk of major adverse events after
116 adjustment for significant stenoses and atherosclerotic cardiovascular disease risk
117 score (HR 1.72, 95% confidence interval [CI] 1.89 – 3.93) (13). Of note, this
118 incremental prognostic power was seen only in patients with non-obstructive
119 disease. In SCOT-HEART, adverse plaque features, present in 608 (34%) patients
120 (40% of patients with non-obstructive plaque and 75% in those with obstructive
121 plaque), conferred a 3-fold higher risk of coronary heart disease death or nonfatal
122 myocardial infarction (HR 3.01, 95% CI 1.61 – 5.63), an effect that was most
123 pronounced during short-term follow-up. The high prevalence of adverse plaque
124 features demonstrates the relatively low positive predictive value of these findings.
125 The prognostic power of adverse plaque features was not independent of coronary
126 artery calcium score, highlighting the importance of total atherosclerotic disease
127 burden. Additionally, approximately half of patients with subsequent adverse events
128 did not have obstructive coronary artery disease, while (14). It is important to note
129 the clinical context of these trials, as vulnerable plaque features may perhaps be
130 more relevant in the acute setting (15) due to the dynamic nature of plaque biology
131 and the increased use of long-term preventative therapies .

132

133 **Cardiovascular magnetic resonance**

134 CMR has become an imaging modality of major interest in recent years as a result of
135 improvements in scanner technology and software. CMR offers a multiparametric
136 approach to cardiovascular imaging, providing unparalleled soft tissue
137 characterisation that is of particular value in the myocardium, alongside information
138 regarding anatomy, function, perfusion and viability. CMR is also able to characterise
139 coronary atherosclerosis, utilising non-contrast T1-weighted (black blood) imaging to
140 detect methaemoglobin found in acute intraplaque haemorrhage or intraluminal
141 thrombosis. High-intensity coronary plaques correlate well with CTCA findings of low
142 attenuation and positive remodelling, demonstrate increased rates of in-situ
143 thrombus, and have been shown to reduce in intensity after statin therapy (16-20).
144 Meanwhile, novel targeted contrast agents have been developed, such as THI0567-
145 targeted liposomal-gadolinium. This agent binds with high affinity to integrin $\alpha 4\beta 1$, a
146 key integrin involved in recruiting inflammatory cells to atherosclerotic plaques, and
147 is able to detect vulnerable aortic plaque in an animal model (21). However, as a
148 result of the inferior spatial resolution compared to CTCA, magnetic resonance
149 coronary angiography (MRCA) is largely restricted to the proximal and mid-vessel
150 coronary segments. Sequences such as the Coronary Atherosclerosis T1-weighted
151 Characterization with integrated anatomical reference (CATCH) (22) have been
152 developed to overcome some of these limitations but remain exploratory at this point
153 in time. The majority of clinical research and histological validation has therefore
154 focused on larger, stationary vessels such as the carotid artery. Longer scan times in
155 comparison to CTCA, cost and accessibility are other potential barriers to wider
156 uptake of CMR for imaging of coronary atherosclerosis.

157

158 **HYBRID IMAGING: DISEASE ACTIVITY**

159 Molecular nuclear imaging techniques utilise targeted probes bound to radioactive
160 isotopes. An understanding of plaque biology and the various components of
161 vulnerable plaque are critical to determine suitable targets for molecular imaging.
162 PET has been studied for many years, primarily in other specialties such as
163 oncology. Coronary PET imaging has previously been limited due to poor spatial
164 resolution, partial volume effects and cardiac motion. However, with improvements in
165 scanners and the development of advanced motion correction and co-registration
166 techniques, many of these limitations have been overcome. There is now major
167 research interest in coronary PET imaging for the assessment of disease activity
168 within atherosclerotic plaques. This interest has led to the advent of bespoke tracers
169 targeting specific aspects of plaque biology to complement the use of more
170 established radiotracers that have been re-purposed from other fields.

171

172 **Positron emission tomography: 18F-fluorodeoxyglucose**

173 18F-fluorodeoxyglucose (18F-FDG) PET has been used widely in oncology for many
174 years and was first utilised to image atherosclerosis in the carotid artery in 2002 (23).
175 As a glucose analogue, it is metabolised and accumulates intracellularly in tissues
176 with high metabolic activity via the glucose transporter protein system. 18F-FDG has
177 therefore been used as a non-specific marker of vascular inflammation in the aorta,
178 carotids and femoral arteries. 18F-FDG uptake has been shown to correlate with the
179 presence of atherosclerosis, features of plaque vulnerability, biomarkers of
180 inflammation (in particular macrophage burden) and clinical cardiovascular risk (24-
181 26).

182

183 Although the ^{18}F -FDG PET is excellent for myocardial viability assessment due to
184 avid uptake in cardiomyocytes, coronary artery uptake is often obscured by the
185 adjacent myocardial signal. This is the main limitation of ^{18}F -FDG for coronary
186 atherosclerosis imaging, even despite dietary restrictions prior to scanning (27-29).
187 ^{18}F -FDG may still prove of value in detecting plaque inflammation in the aorta and
188 carotid arteries; large prospective outcome studies are awaited.

189

190 **Positron emission tomography: ^{18}F -sodium fluoride**

191 Given ^{18}F -FDG's lack of specificity, other radiotracers have been explored. ^{18}F -
192 sodium fluoride (^{18}F -NaF) has been used as a bone tracer and for the detection of
193 bony metastases for many decades but has now found a potential application in
194 hybrid cardiac imaging. The ligand for ^{18}F -NaF is hydroxyapatite, a key component
195 of early bone and vascular calcification. It preferentially binds to micro- rather than
196 macrocalcification due to the higher exposed surface area of hydroxyapatite (30).
197 Microcalcification is thought to be an early healing response to cell necrosis and
198 inflammation that precedes the development of larger, macroscopic deposits of
199 calcium which can stabilise plaque. Microcalcification within a thin fibrous cap may
200 also increase local stress and destabilize the plaque, thereby increasing the chance
201 of rupture (31). Coronary microcalcification is therefore a key component of
202 vulnerable plaque and a biologically plausible target for imaging, with ^{18}F -NaF
203 providing different information to the more established, stable macrocalcification
204 identified on CT.

205

206 ^{18}F -NaF PET-CT was noted to identify aortic plaque in 2010 (32). Subsequent data
207 has shown that increased ^{18}F -NaF activity can be identified in the coronary arteries,

208 localising to individual plaques and demonstrating excellent inter-observer
209 repeatability (33). This improved ability to detect discrete coronary artery uptake
210 compared to ^{18}F -FDG appears to be due to low ^{18}F -NaF uptake in the adjacent
211 myocardium and very high affinity of the tracer for microcalcification (30, 34) Again,
212 ^{18}F -NaF appears to be providing different information to the presence of calcium on
213 CT; in one study, almost a half of patients with a calcium score >1000 Agatston
214 units did not have any coronary ^{18}F -NaF uptake (33). In keeping with the hypothesis
215 that ^{18}F -NaF uptake is associated with vulnerable plaque, several clinical studies
216 have demonstrated uptake to be associated with culprit and high-risk coronary
217 plaque as defined by invasive angiography, intravascular ultrasound and CTCA. In
218 the first report, increased ^{18}F -fluoride uptake was observed at the site of the culprit
219 coronary plaque in 37 of the 40 patients with recent myocardial infarction (29), a
220 finding supported by two subsequent smaller studies (35, 36).

221

222 Recent technological advances have greatly improved the image quality of coronary
223 ^{18}F -NaF PET-CT imaging. These techniques have focused on optimizing image
224 reconstruction and correcting for cardiac, respiratory and gross patient motion, with
225 the important advantage that they can be applied retrospectively to PET datasets
226 (37-39). Newer data have also demonstrated the feasibility of fusing PET data with
227 previously acquired CTCA, expanding the potential practical application of this form
228 of imaging (40). ^{18}F -NaF PET-MR is also feasible with lower doses of ionising
229 radiation, but currently cannot provide the spatial resolution of CTCA for coronary
230 artery imaging (41).

231

232 **Positron emission tomography: other radiotracers**

233 Multiple alternative radiotracers, each with a specific target, have been studied for
234 use in atherosclerosis (Table 1) (42). ⁶⁸Ga-DOTATATE, which targets the
235 somatostatin receptor subtype 2 (SSTR2) on the surface of activated
236 proinflammatory M1 macrophages, has recently been investigated for coronary
237 atherosclerosis imaging. The Vascular Inflammation imaging using Somatostatin
238 receptor positron emission tomography (VISION) study utilised RNA sequencing,
239 autoradiology, histology and PET-CT in patients with stable and unstable
240 cardiovascular disease. The investigators elegantly demonstrated exclusive
241 expression of SSTR2 in M1 macrophages within atherosclerotic plaque, a strong
242 correlation between SSTR2 expression and ⁶⁸Ga-DOTATATE activity, and
243 improved discrimination of culprit and high-risk plaque in both the coronary and
244 carotid arteries compared to ¹⁸F-FDG (43). Further studies are keenly anticipated.
245 Other examples of alternative radiotracers include ¹¹C-PK11195, which is a specific
246 ligand of the translocator protein that is highly expressed on activated phagocytes,
247 and the chemokine receptor CXCR4, which is upregulated in unstable plaque and
248 colocalizes with CD68 inflammatory cells. ¹¹C-PK11195 is able to image intraplaque
249 haemorrhage in recently symptomatic carotid plaques (44) as well as active disease
250 in large-vessel vasculitis, while CXCR4 has recently shown promise for the
251 distinguishing culprit and non-culprit coronary plaques in ST-elevation myocardial
252 infarction (45).

253

254 **HYBRID IMAGING: PHYSIOLOGY**

255 In addition to measurements of plaque composition and disease activity, PET/CT
256 also allows for functional assessments of atherosclerotic lesions, whether using
257 myocardial perfusion studies or non-invasive fraction flow reserve (FFR). This is of

258 interest as recent data have suggested that vulnerable plaque characteristics are
259 associated with haemodynamically significant lesions, and that integrating luminal
260 stenosis, adverse plaque characteristics and adverse haemodynamic characteristics
261 (comprised of CT-derived FFR (CT-FFR), delta CT-FFR across the vessel, wall
262 shear stress and axial plaque stress) provides better identification of culprit lesions
263 than each individual parameter (46). Functional coronary assessments may
264 therefore act as both surrogates of adverse plaque features, as well as an additional
265 modality to add incremental prognostic information.

266

267 With invasive FFR now routinely used for decision making in interventional
268 cardiology, interest has grown in the potential for CT-FFR to enhance the role of
269 CTCA as a gatekeeper to invasive angiography. Although CT-FFR does not image
270 vulnerable plaque directly, several studies have demonstrated that CTCA
271 assessments of plaque composition improve discrimination of ischaemic lesions as
272 defined by an invasive FFR ≤ 0.80 or by decreased quantitative myocardial blood
273 flow (47-51). The number of adverse plaque features appear to increase as stenosis
274 severity increase, but the presence of high-risk plaque also remains an independent
275 predictor of ischaemia regardless of stenosis severity, particularly positive
276 remodelling (47, 48, 51). The mechanisms for these findings are not clear but reflect
277 the complex relationship between coronary atherosclerosis and ischemia. Positive
278 remodelling and the lipid-rich necrotic core of the vulnerable plaque may predispose
279 to local endothelial dysfunction and altered shear stress, thus altering impairing
280 arterial vasomotor function. This hypothesis is supported by a recent exploratory
281 study in which high-risk plaque characteristics were more strongly related to invasive
282 pressure measurements during hyperaemia than during rest (52). The adaptive

283 arterial remodelling response to the progression of atheroma – the Glagov
284 phenomenon – may also reach its limit with a certain volume of plaque, at which
285 point luminal encroachment, obstruction to flow and ischaemia may rapidly progress
286 (53).

287

288 PET provides the gold standard non-invasive assessment of myocardial perfusion.
289 Unlike FFR, PET is able to provide a quantitative assessment of absolute
290 hyperaemic blood flow and myocardial blood flow reserve, thus integrating the
291 combined effect of epicardial coronary arterial atherosclerosis as well as
292 microvascular disease. The Prospective Comparison of Cardiac PET/CT, SPECT/CT
293 Perfusion Imaging and CT Coronary Angiography With Invasive Coronary
294 Angiography (PACIFIC) study demonstrated PET to be superior to CTCA and single-
295 photon emission computed tomography (SPECT) for the diagnosis of ischaemia
296 (based on invasive FFR) (54). Although this study showed only limited additional
297 diagnostic value with hybrid imaging, a recent meta-analysis confirmed incremental
298 diagnostic performance with hybrid anatomy/perfusion imaging compared to CTCA
299 (55). Additionally, several retrospective studies consistently described an
300 incremental prognostic value of combining myocardial perfusion imaging and CTCA
301 (56, 57). Further data is now needed to investigate the association between adverse
302 plaque features and myocardial perfusion on PET, to assess whether the latter might
303 also provide a surrogate for unstable coronary plaque phenotypes.

304

305 The future of non-invasive coronary anatomy/physiology imaging is therefore
306 extremely promising; there is great appeal in deriving a hybrid dataset assessing

307 coronary anatomy, plaque morphology, plaque burden and coronary flow at both a
308 lesion and vessel level. Randomized clinical trials will be highly anticipated.

309

310 **CURRENT LIMITATIONS**

311 Although the appeal of hybrid imaging is clear, there remain some limitations. Most
312 crucially, until recently there has been a lack of randomised data demonstrating the
313 ability of these imaging techniques to change outcomes. We now have this data
314 supporting the use of CTCA, but there is a major need for similar data demonstrating
315 the benefits of hybrid non-invasive ischaemia testing. Furthermore, access to
316 scanners and integration of these imaging techniques into clinical workflows in
317 imaging departments must be considered. Costs is also an issue, particularly with
318 regards to the production of bespoke radiotracers for nuclear imaging. Consequently,
319 which test to use in which patients in what setting must be carefully considered,
320 taking into account all of these factors. This is in addition to other clinical factors that
321 may influence the choice of test, such as patient age, likelihood of calcific disease,
322 ability to achieve adequate heart rate control, comorbidities and acceptable radiation
323 dose.

324

325 **CASE 1**

326 A 57-year-old man with type 2 diabetes mellitus presented with a non-ST elevation
327 myocardial infarction (NSTEMI) and underwent percutaneous coronary intervention
328 with two drug-eluting stents to the proximal right coronary artery (RCA) and posterior
329 left ventricular artery (PLV). Six months later, he re-presented with another NSTEMI
330 despite appropriate preventative therapies. Invasive coronary angiography
331 demonstrated severe in-stent restenosis in the proximal stent and a further severe

332 de novo mid-RCA (Figure 1A). Optical coherence tomography demonstrated plaque
333 rupture with red thrombus in the mid-vessel lesion and aggressive neointimal
334 hyperplasia in the proximal lesion (Figure 1B-C). Two drug-eluting stents were
335 implanted with a good angiographic result (Figure 1D). The left system, particularly
336 the left anterior descending artery (LAD), had diffuse plaque without obstructive
337 disease (Figure 1E). As part of a research study, the patient underwent ¹⁸F-NaF
338 PET-CT six weeks later. This demonstrated three discrete regions of focal uptake in
339 the proximal, mid and distal RCA (arrows). Although the mid-RCA lesion was the
340 culprit, the highest uptake was in the proximal restenotic lesion. In contrast to the
341 RCA, the diffusely diseased LAD had non-obstructive calcific plaque without high-
342 risk features on CTCA and did not demonstrate any ¹⁸F-NaF uptake (Figure 1F).

343

344 **CASE 2**

345 A patient was referred three weeks after an episode of chest pain with a late
346 presentation myocardial infarction. He was not revascularized due to established
347 infarction. Six months post-infarct, he underwent ¹⁸F-NaF PET-MR. Whole-heart, 3-
348 dimensional, contrast-enhanced coronary MR angiography using a respiratory-
349 navigated, electrocardiographically triggered, inversion-recovery fast spoiled
350 gradient-echo sequence demonstrated a severe culprit plaque in the proximal LAD
351 (Figure 1A). Extensive near-transmural infarction in this territory was seen on late
352 gadolinium enhancement (Figure 1B). Focal ¹⁸F-NaF uptake was noted in the culprit
353 lesion (Figure 1C-D, white arrowheads) as well as in the aorta and mitral annulus
354 (black arrows). Adapted from Robson *et al* (41).

355

356 **CONCLUSIONS**

357 The field of cardiovascular atherosclerosis imaging is burgeoning, with increasing
358 availability and uptake of CT and CMR in particular. Hybrid imaging platforms
359 combine these modalities with PET, which together provide detailed information
360 about coronary anatomy, flow, plaque morphology and disease activity, potentially
361 expanding our pathophysiological understanding of atherosclerosis and improving
362 risk stratification. Further studies are now required to investigate the clinical utility of
363 this approach and determine whether hybrid imaging of the vulnerable plaque can
364 improve patient outcomes.

365

366 **FUNDING**

367 Dr Marc Dweck is supported by a BHF Intermediate Clinical Research Fellowship

368 Grant (FS/14/78/31020).

369

370

371

372

ACCEPTED MANUSCRIPT

373 **REFERENCES**

374

- 375 1. GBD Causes of Death Collaborators. Global, regional, and national age-sex
376 specific mortality for 264 causes of death, 1980-2016: a systematic analysis for the
377 Global Burden of Disease Study 2016. *Lancet*. 2017;390(10100):1151-210.
- 378 2. Virmani R, Burke AP, Farb A, Kolodgie FD. Pathology of the vulnerable
379 plaque. *J Am Coll Cardiol*. 2006;47(8 Suppl):C13-8.
- 380 3. Arbab-Zadeh A, Fuster V. The myth of the "vulnerable plaque": transitioning
381 from a focus on individual lesions to atherosclerotic disease burden for coronary
382 artery disease risk assessment. *J Am Coll Cardiol*. 2015;65(8):846-55.
- 383 4. Stone GW, Maehara A, Lansky AJ, de Bruyne B, Cristea E, Mintz GS, et al. A
384 prospective natural-history study of coronary atherosclerosis. *N Engl J Med*.
385 2011;364(3):226-35.
- 386 5. Chang HJ, Lin FY, Lee SE, Andreini D, Bax J, Cademartiri F, et al. Coronary
387 Atherosclerotic Precursors of Acute Coronary Syndromes. *J Am Coll Cardiol*.
388 2018;71(22):2511-22.
- 389 6. Waksman R, editor *Assessment of Coronary Near-Infrared Spectroscopy*
390 *Imaging to Detect Vulnerable Plaques and Vulnerable Patients; The Lipid-Rich*
391 *Plaque Study*. Transcatheter Cardiovascular Therapeutics; 2018 24/9/2018; San
392 Diego, California.
- 393 7. Tanaka A, Shimada K, Yoshida K, Jissyo S, Tanaka H, Sakamoto M, et al.
394 Non-invasive assessment of plaque rupture by 64-slice multidetector computed
395 tomography--comparison with intravascular ultrasound. *Circulation journal : official*
396 *journal of the Japanese Circulation Society*. 2008;72(8):1276-81.

- 397 8. Kashiwagi M, Tanaka A, Kitabata H, Tsujioka H, Kataiwa H, Komukai K, et al.
398 Feasibility of noninvasive assessment of thin-cap fibroatheroma by multidetector
399 computed tomography. *JACC Cardiovascular imaging*. 2009;2(12):1412-9.
- 400 9. Motoyama S, Kondo T, Sarai M, Sugiura A, Harigaya H, Sato T, et al.
401 Multislice computed tomographic characteristics of coronary lesions in acute
402 coronary syndromes. *J Am Coll Cardiol*. 2007;50(4):319-26.
- 403 10. Motoyama S, Ito H, Sarai M, Kondo T, Kawai H, Nagahara Y, et al. Plaque
404 Characterization by Coronary Computed Tomography Angiography and the
405 Likelihood of Acute Coronary Events in Mid-Term Follow-Up. *J Am Coll Cardiol*.
406 2015;66(4):337-46.
- 407 11. Motoyama S, Sarai M, Harigaya H, Anno H, Inoue K, Hara T, et al. Computed
408 Tomographic Angiography Characteristics of Atherosclerotic Plaques Subsequently
409 Resulting in Acute Coronary Syndrome. *Journal of the American College of*
410 *Cardiology*. 2009;54(1):49-57.
- 411 12. Yamamoto H, Kihara Y, Kitagawa T, Ohashi N, Kunita E, Iwanaga Y, et al.
412 Coronary plaque characteristics in computed tomography and 2-year outcomes: The
413 PREDICT study. *Journal of cardiovascular computed tomography*. 2018;12(5):436-
414 43.
- 415 13. Ferencik M, Mayrhofer T, Bittner DO, Emami H, Puchner SB, Lu MT, et al.
416 Use of High-Risk Coronary Atherosclerotic Plaque Detection for Risk Stratification of
417 Patients With Stable Chest Pain: A Secondary Analysis of the PROMISE
418 Randomized Clinical Trial. *JAMA Cardiol*. 2018;3(2):144-52.
- 419 14. Williams M, Moss A, Dweck M, Adamson P, Alam S, Hunter A, et al. Coronary
420 artery plaque characteristics associated with adverse outcomes in the SCOT-HEART
421 study. *Journal of the American College of Cardiology*. 2019;73(3. In press.).

- 422 15. Puchner SB, Liu T, Mayrhofer T, Truong QA, Lee H, Fleg JL, et al. High-risk
423 plaque detected on coronary CT angiography predicts acute coronary syndromes
424 independent of significant stenosis in acute chest pain: results from the ROMICAT-II
425 trial. *Journal of the American College of Cardiology*. 2014;64(7):684-92.
- 426 16. Kawasaki T, Koga S, Koga N, Noguchi T, Tanaka H, Koga H, et al.
427 Characterization of hyperintense plaque with noncontrast T(1)-weighted cardiac
428 magnetic resonance coronary plaque imaging: comparison with multislice computed
429 tomography and intravascular ultrasound. *JACC Cardiovascular imaging*.
430 2009;2(6):720-8.
- 431 17. Matsumoto K, Ehara S, Hasegawa T, Sakaguchi M, Otsuka K, Yoshikawa J,
432 et al. Localization of Coronary High-Intensity Signals on T1-Weighted MR Imaging:
433 Relation to Plaque Morphology and Clinical Severity of Angina Pectoris. *JACC*
434 *Cardiovascular imaging*. 2015;8(10):1143-52.
- 435 18. Noguchi T, Tanaka A, Kawasaki T, Goto Y, Morita Y, Asaumi Y, et al. Effect of
436 Intensive Statin Therapy on Coronary High-Intensity Plaques Detected by
437 Noncontrast T1-Weighted Imaging: The AQUAMARINE Pilot Study. *Journal of the*
438 *American College of Cardiology*. 2015;66(3):245-56.
- 439 19. Oshita A, Kawakami H, Miyoshi T, Seike F, Matsuoka H. Characterization of
440 high-intensity plaques on noncontrast T1-weighted magnetic resonance imaging by
441 coronary angiography. *Journal of cardiology*. 2017;70(6):520-3.
- 442 20. Matsumoto K, Ehara S, Hasegawa T, Nishimura S, Shimada K. The signal
443 intensity of coronary culprit lesions on T1-weighted magnetic resonance imaging is
444 directly correlated with the accumulation of vulnerable morphologies. *International*
445 *journal of cardiology*. 2017;231:284-6.

- 446 21. Woodside DG, Tanifum EA, Ghaghada KB, Biediger RJ, Caivano AR,
447 Starosolski ZA, et al. Magnetic Resonance Imaging of Atherosclerotic Plaque at
448 Clinically Relevant Field Strengths (1T) by Targeting the Integrin $\alpha_4\beta_1$.
449 Scientific reports. 2018;8(1):3733.
- 450 22. Xie Y, Kim YJ, Pang J, Kim JS, Yang Q, Wei J, et al. Coronary
451 Atherosclerosis T1-Weighted Characterization With Integrated Anatomical Reference:
452 Comparison With High-Risk Plaque Features Detected by Invasive Coronary
453 Imaging. JACC Cardiovascular imaging. 2017;10(6):637-48.
- 454 23. Rudd JH, Warburton EA, Fryer TD, Jones HA, Clark JC, Antoun N, et al.
455 Imaging atherosclerotic plaque inflammation with [18F]-fluorodeoxyglucose positron
456 emission tomography. Circulation. 2002;105(23):2708-11.
- 457 24. Silvera SS, Aidi HE, Rudd JH, Mani V, Yang L, Farkouh M, et al. Multimodality
458 imaging of atherosclerotic plaque activity and composition using FDG-PET/CT and
459 MRI in carotid and femoral arteries. Atherosclerosis. 2009;207(1):139-43.
- 460 25. Tarkin JM, Joshi FR, Rudd JH. PET imaging of inflammation in
461 atherosclerosis. Nature reviews Cardiology. 2014;11(8):443-57.
- 462 26. Joshi NV, Toor I, Shah AS, Carruthers K, Vesey AT, Alam SR, et al. Systemic
463 Atherosclerotic Inflammation Following Acute Myocardial Infarction: Myocardial
464 Infarction Begets Myocardial Infarction. Journal of the American Heart Association.
465 2015;4(9):e001956.
- 466 27. Wykrzykowska J, Lehman S, Williams G, Parker JA, Palmer MR, Varkey S, et
467 al. Imaging of inflamed and vulnerable plaque in coronary arteries with 18F-FDG
468 PET/CT in patients with suppression of myocardial uptake using a low-carbohydrate,
469 high-fat preparation. Journal of nuclear medicine : official publication, Society of
470 Nuclear Medicine. 2009;50(4):563-8.

- 471 28. Rogers IS, Nasir K, Figueroa AL, Cury RC, Hoffmann U, Vermylen DA, et al.
472 Feasibility of FDG Imaging of the Coronary Arteries: Comparison Between Acute
473 Coronary Syndrome and Stable Angina. *JACC: Cardiovascular Imaging*.
474 2010;3(4):388-97.
- 475 29. Joshi NV, Vesey AT, Williams MC, Shah AS, Calvert PA, Craighead FH, et al.
476 ¹⁸F-fluoride positron emission tomography for identification of ruptured and high-risk
477 coronary atherosclerotic plaques: a prospective clinical trial. *Lancet*.
478 2014;383(9918):705-13.
- 479 30. Creager MD, Hohl T, Hutcheson JD, Moss AJ, Schlotter F, Blaser MC, et al.
480 (18)F-Fluoride Signal Amplification Identifies Microcalcifications Associated With
481 Atherosclerotic Plaque Instability in Positron Emission Tomography/Computed
482 Tomography Images. *Circ Cardiovasc Imaging*. 2019;12(1):e007835.
- 483 31. Hutcheson JD, Maldonado N, Aikawa E. Small entities with large impact:
484 microcalcifications and atherosclerotic plaque vulnerability. *Current opinion in*
485 *lipidology*. 2014;25(5):327-32.
- 486 32. Derlin T, Richter U, Bannas P, Begemann P, Buchert R, Mester J, et al.
487 Feasibility of ¹⁸F-sodium fluoride PET/CT for imaging of atherosclerotic plaque.
488 *Journal of nuclear medicine : official publication, Society of Nuclear Medicine*.
489 2010;51(6):862-5.
- 490 33. Dweck MR, Chow MW, Joshi NV, Williams MC, Jones C, Fletcher AM, et al.
491 Coronary arterial ¹⁸F-sodium fluoride uptake: a novel marker of plaque biology. *J*
492 *Am Coll Cardiol*. 2012;59(17):1539-48.
- 493 34. Irkle A, Vesey AT, Lewis DY, Skepper JN, Bird JL, Dweck MR, et al.
494 Identifying active vascular microcalcification by (18)F-sodium fluoride positron
495 emission tomography. *Nature communications*. 2015;6:7495.

- 496 35. Marchesseau S, Seneviratna A, Sjöholm AT, Qin DL, Ho JXM, Hausenloy DJ,
497 et al. Hybrid PET/CT and PET/MRI imaging of vulnerable coronary plaque and
498 myocardial scar tissue in acute myocardial infarction. *J Nucl Cardiol*.
499 2017;10.1007/s12350-017-0918-8.
- 500 36. Kitagawa T, Yamamoto H, Nakamoto Y, Sasaki K, Toshimitsu S, Tatsugami
501 F, et al. Predictive Value of (18)F-Sodium Fluoride Positron Emission Tomography in
502 Detecting High-Risk Coronary Artery Disease in Combination With Computed
503 Tomography. *Journal of the American Heart Association*. 2018;7(20):e010224.
- 504 37. Rubeaux M, Joshi NV, Dweck MR, Fletcher A, Motwani M, Thomson LE, et al.
505 Motion Correction of 18F-NaF PET for Imaging Coronary Atherosclerotic Plaques.
506 *Journal of nuclear medicine : official publication, Society of Nuclear Medicine*.
507 2016;57(1):54-9.
- 508 38. Doris MK, Otaki Y, Krishnan SK, Kwiecinski J, Rubeaux M, Alessio A, et al.
509 Optimization of reconstruction and quantification of motion-corrected coronary PET-
510 CT. *J Nucl Cardiol*. 2018;10.1007/s12350-018-1317-5.
- 511 39. Lassen ML, Kwiecinski J, Cadet S, Dey D, Wang C, Dweck MR, et al. Data-
512 driven gross patient motion detection and compensation: Implications for coronary
513 (18)F-NaF PET imaging. *Journal of nuclear medicine : official publication, Society of*
514 *Nuclear Medicine*. 2018;10.2967/jnumed.118.217877.
- 515 40. Kwiecinski J, Adamson PD, Lassen ML, Doris MK, Moss AJ, Cadet S, et al.
516 Feasibility of Coronary (18)F-Sodium Fluoride Positron-Emission Tomography
517 Assessment With the Utilization of Previously Acquired Computed Tomography
518 Angiography. *Circ Cardiovasc Imaging*. 2018;11(12):e008325.

- 519 41. Robson PM, Dweck MR, Trivieri MG, Abgral R, Karakatsanis NA, Contreras J,
520 et al. Coronary Artery PET/MR Imaging: Feasibility, Limitations, and Solutions. *JACC*
521 *Cardiovascular imaging*. 2017;10(10 Pt A):1103-12.
- 522 42. Andrews JPM, Fayad ZA, Dweck MR. New methods to image unstable
523 atherosclerotic plaques. *Atherosclerosis*. 2018;272:118-28.
- 524 43. Tarkin JM, Joshi FR, Evans NR, Chowdhury MM, Figg NL, Shah AV, et al.
525 Detection of Atherosclerotic Inflammation by (68)Ga-DOTATATE PET Compared to
526 [(18)F]FDG PET Imaging. *J Am Coll Cardiol*. 2017;69(14):1774-91.
- 527 44. Gaemperli O, Shalhoub J, Owen DR, Lamare F, Johansson S, Fouladi N, et
528 al. Imaging intraplaque inflammation in carotid atherosclerosis with 11C-PK11195
529 positron emission tomography/computed tomography. *Eur Heart J*.
530 2012;33(15):1902-10.
- 531 45. Derlin T, Sedding DG, Dutzmann J, Haghikia A, König T, Napp LC, et al.
532 Imaging of chemokine receptor CXCR4 expression in culprit and nonculprit coronary
533 atherosclerotic plaque using motion-corrected [68Ga]pentixafor PET/CT. *European*
534 *journal of nuclear medicine and molecular imaging*. 2018;45(11):1934-44.
- 535 46. Lee JM, Choi G, Koo BK, Hwang D, Park J, Zhang J, et al. Identification of
536 High-Risk Plaques Destined to Cause Acute Coronary Syndrome Using Coronary
537 Computed Tomographic Angiography and Computational Fluid Dynamics. *JACC*
538 *Cardiovascular imaging*. 2018;10.1016/j.jcmg.2018.01.023.
- 539 47. Park H-B, Heo R, ó Hartaigh B, Cho I, Gransar H, Nakazato R, et al.
540 Atherosclerotic Plaque Characteristics by CT Angiography Identify Coronary Lesions
541 That Cause Ischemia: A Direct Comparison to Fractional Flow Reserve. *JACC:*
542 *Cardiovascular Imaging*. 2015;8(1):1-10.

- 543 48. Nakazato R, Park H-B, Gransar H, Leipsic JA, Budoff MJ, Mancini GBJ, et al.
544 Additive diagnostic value of atherosclerotic plaque characteristics to non-invasive
545 FFR for identification of lesions causing ischaemia: results from a prospective
546 international multicentre trial. *EuroIntervention*. 2016;12(4):473-81.
- 547 49. Gaur S, Øvrehus KA, Dey D, Leipsic J, Bøtker HE, Jensen JM, et al. Coronary
548 plaque quantification and fractional flow reserve by coronary computed tomography
549 angiography identify ischaemia-causing lesions. *European Heart Journal*.
550 2016;37(15):1220-7.
- 551 50. Ovrehus KA, Gaur S, Leipsic J, Jensen JM, Dey D, Botker HE, et al. CT-
552 based total vessel plaque analyses improves prediction of hemodynamic significance
553 lesions as assessed by fractional flow reserve in patients with stable angina pectoris.
554 *Journal of cardiovascular computed tomography*. 2018;12(4):344-9.
- 555 51. Driessen RS, Stuijzand WJ, Raijmakers PG, Danad I, Min JK, Leipsic JA, et
556 al. Effect of Plaque Burden and Morphology on Myocardial Blood Flow and
557 Fractional Flow Reserve. *J Am Coll Cardiol*. 2018;71(5):499-509.
- 558 52. Driessen RS, Stuijzand WJ, Raijmakers PG, Danad I, Min JK, Leipsic JA, et
559 al. Vulnerable plaques are revealed by fractional flow reserve but not by
560 instantaneous wave-free ratio. *European Heart Journal*. 2018;39(suppl_1).
- 561 53. Narula J, Nakano M, Virmani R, Kolodgie FD, Petersen R, Newcomb R, et al.
562 Histopathologic characteristics of atherosclerotic coronary disease and implications
563 of the findings for the invasive and noninvasive detection of vulnerable plaques. *J*
564 *Am Coll Cardiol*. 2013;61(10):1041-51.
- 565 54. Danad I, Raijmakers PG, Driessen RS, Leipsic J, Raju R, Naoum C, et al.
566 Comparison of Coronary CT Angiography, SPECT, PET, and Hybrid Imaging for

- 567 Diagnosis of Ischemic Heart Disease Determined by Fractional Flow Reserve. JAMA
568 Cardiol. 2017;2(10):1100-7.
- 569 55. Rizvi A, Han D, Danad I, B OH, Lee JH, Gransar H, et al. Diagnostic
570 Performance of Hybrid Cardiac Imaging Methods for Assessment of Obstructive
571 Coronary Artery Disease Compared With Stand-Alone Coronary Computed
572 Tomography Angiography: A Meta-Analysis. JACC Cardiovascular imaging.
573 2018;11(4):589-99.
- 574 56. Pazhenkottil AP, Benz DC, Gräni C, Madsen MA, Mikulicic F, von Felten E, et
575 al. Hybrid SPECT Perfusion Imaging and Coronary CT Angiography: Long-term
576 Prognostic Value for Cardiovascular Outcomes. Radiology. 2018;288(3):694-702.
- 577 57. Maaniitty T, Stenstrom I, Bax JJ, Uusitalo V, Ukkonen H, Kajander S, et al.
578 Prognostic Value of Coronary CT Angiography With Selective PET Perfusion
579 Imaging in Coronary Artery Disease. JACC Cardiovascular imaging.
580 2017;10(11):1361-70.

FIGURE LEGENDS**Figure 1**

Invasive angiography (A, D, E), optical coherence tomography (B, C) and positron emission tomography-computed tomography (F, G) for Case 1. Descriptions provided in case vignette.

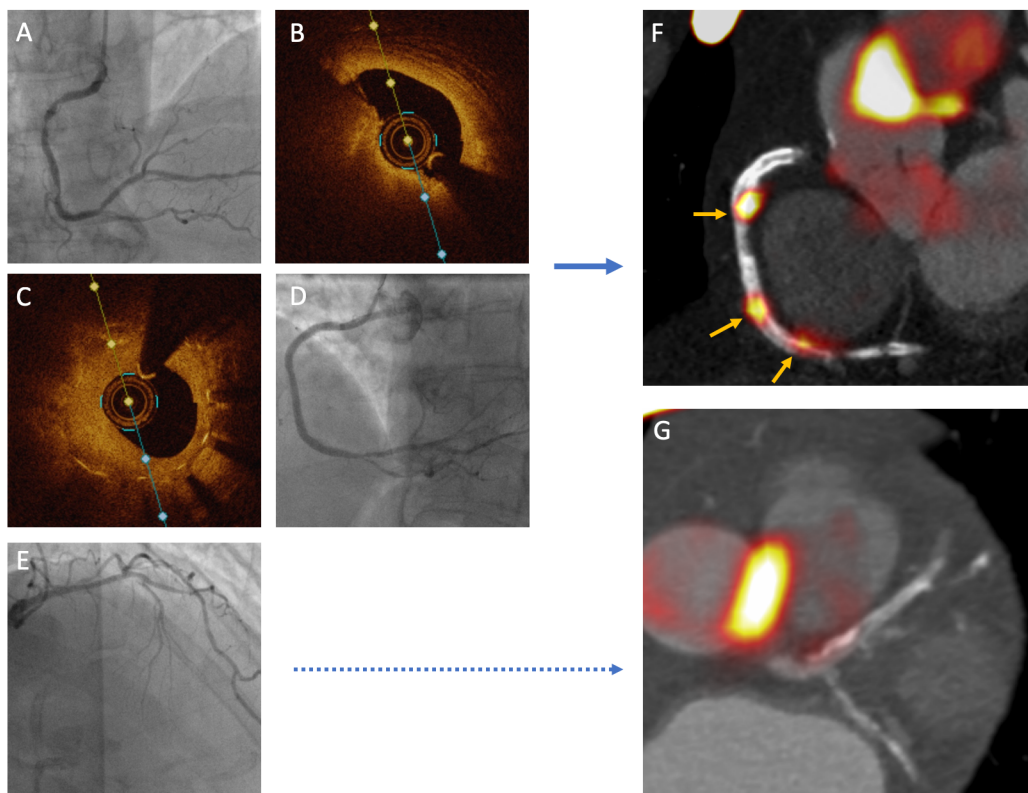
Figure 2

Cardiac magnetic resonance for Case 2. Descriptions provided in case vignette.

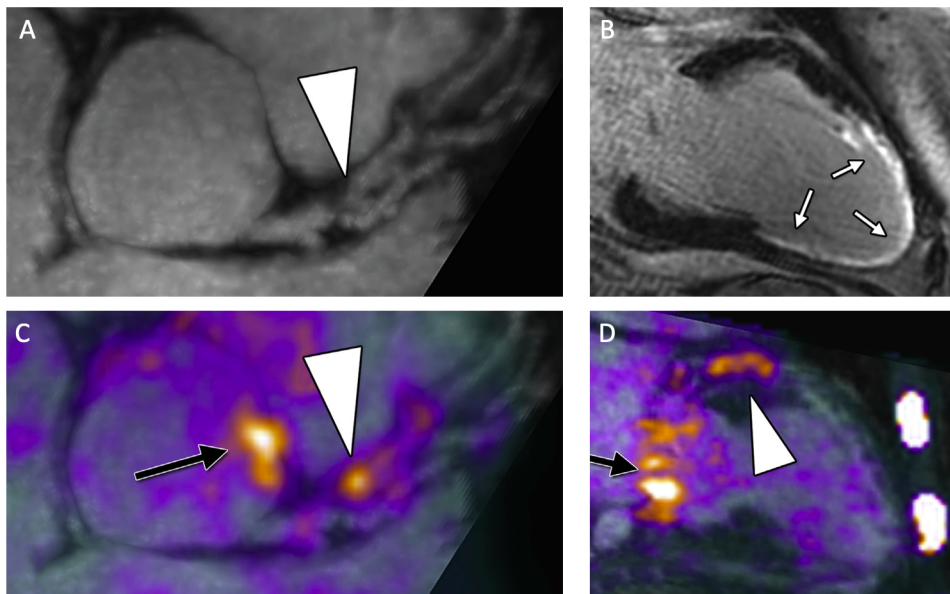
Table 1 Positron emission tomography radiotracers targeting vulnerable plaque

Target	Ligand	Radiotracer	Current applications in atherosclerosis
Macrophage activation	Glucose transporter protein system. Conversion to 18F-FDG-6-phosphate and intracellular accumulation	¹⁸ F-FDG	Prospective <i>in vivo</i> studies in extracardiac atherosclerosis. Correlation with atherosclerosis and cardiovascular risk. Myocardial signal spill-over limits coronary artery assessment (35, 37).
	Somatostatin receptor subtype 2	⁶⁸ Ga-DOTATATE	Prospective <i>in vivo</i> studies in cardiac and extracardiac atherosclerosis. Correlation with culprit coronary lesions and high-risk features on CTCA (52).
	Translocator protein 18-kDa	¹¹ C-PK11195	Prospective <i>in vivo</i> study in carotid atherosclerosis (67). Short half-life and variable metabolism.
	Choline kinase phosphorylated to phosphatidylcholine	¹⁸ F-FCH	Retrospective <i>in vivo</i> study demonstrating correlation with large vessel atherosclerosis and an inverse relationship with calcification (68).
Apoptosis	Phosphatidylserine	Annexin V	Prospective <i>in vivo</i> pilot data in carotid atherosclerosis (69).
Hypoxia	Reduction to amine derivative in low oxygen environment	¹⁸ F-FMISO	Prospective <i>in vivo</i> pilot data in carotid atherosclerosis (70).
	Reduction to amine derivative in low O ₂ environment	¹⁸ F-HX4	Prospective <i>in vivo</i> pilot data in carotid atherosclerosis (71).
Microcalcification	Hydroxyapatite	¹⁸ F-NaF	Prospective <i>in vivo</i> studies in coronary and extracardiac atherosclerosis. Correlation with culprit coronary lesions and high-risk features on CTCA (37, 41, 44, 72).
Angiogenesis	αVβ3 & αVβ5 integrin	¹⁸ F-Fluciclatide	Prospective <i>in vivo</i> pilot data in the aorta (73).
	αVβ3 integrin	¹⁸ F-RGD-K5	<i>Ex vivo</i> study in carotid atherosclerosis (74).
Thrombus	Glycoprotein IIb/IIIa platelet receptor	¹⁸ F-GP1	Prospective <i>in vivo</i> pilot data in arterial thromboembolic disease (75).

¹⁸F-FDG: 18-fluorodeoxyglucose, CTCA: computed tomography coronary angiography, ¹⁸F-FCH: 18F-fluorocholine, ¹⁸F-FMISO: 18F-fluoromisonidazole, ¹⁸F-HX4: 18F-2-(4-((2-nitro-1H-imidazol-1-yl)methyl)-1H-1,2,3-triazol-1-yl)propan-1-ol, ¹⁸F-NaF: 18F-sodium fluoride, ¹⁸F-RGD-K5: arginine-glycine-aspartate-K5.



ACCEPTED MANUSCRIPT



ACCEPTED MANUSCRIPT